Turkish Journal of Agriculture - Food Science and Technology, 12(4): 692-698, 2024
DOI: https://doi.org/10.24925/turjaf.v12i4.692-698.6620

Turkish Journal of Agriculture - Food Science and Technology

Available online, ISSN: 2148-127X | www.agrifoodscience.com | Turkish Science and Technology Publishing (TURSTEP)

Electrochemical Non-Enzymatic Glucose Sensing Platform Based on Vanadium Pentoxide Film-Modified Screen Printed Gold Electrode

Çiğdem Dülgerbaki[1,a,*]

[1] *Alanya Alaaddin Keykubat University, Faculty of Engineering, Department of Engineering Fundamental Sciences, Alanya, Antalya, Türkiye*
[*] *Corresponding author*

ARTICLE INFO

Research Article

Received : 22.12.2023
Accepted : 18.03.2024

Keywords:
Vanadium pentoxide
Glucose
Biosensor
Electrodeposition
Screen printed gold electrode

ABSTRACT

A screen printed gold electrode (SPGE) served as the foundation for directly depositing Vanadium pentoxide (V_2O_5), crafting an enzyme-free glucose sensor. Through cyclic voltammetry in an alkaline setting, the sensor's ability to drive glucose oxidation was explored. Utilizing V_2O_5 as an electrocatalyst, this non-enzymatic sensor exhibited an expansive linear detection range (1 mM–10 mM) and an impressively low detection limit of 0.9 µM. These results underscored V_2O_5's robust electrocatalytic process in facilitating glucose oxidation within alkaline solutions, unaffected notably by substances like ascorbic acid, fructose and maltose. This investigation highlights a direct and efficient method for glucose detection without reliance on enzymes.

[a] *cigdem.dulgerbaki@alanya.edu.tr* *https://orcid.org/0000-0001-6426-7220*

Introduction

D-Glucose (DGLC) acts as the main energy source for the human body and plays a role in forming metabolic intermediates. However, deviations in DGLC levels in the bloodstream are associated with diabetes mellitus (Rahman et al., 2019). Regardless of socioeconomic status, diabetes has notably surged in many middle-income countries across the globe. Although chronic, diabetes can lead to severe complications and symptoms such as cardiac issues, blindness, ocular problems, peripheral vascular diseases, strokes and kidney failure. The body typically maintains blood DGLC levels within a range of 70–120 $mgdL^{-1}$. Diabetic individuals often exhibit significantly elevated DGLC levels due to their inability to regulate their sugar levels (Razak et al., 2016). Extensive research in diabetes management shows that closely watching blood glucose levels can postpone the development and advancement of complications associated with diabetes (Dong et al., 2021).

Accurate measurement of glucose holds significance in diverse sectors such as the food industry, fuel cells, environmental studies and pharmaceuticals. Given the myriad applications of glucose, multiple detection methods have been employed to quantify it (Dhara and Mahapatra, 2018). Various conventional approaches, including chromatographic (Filip et al., 2016), spectrophotometric (Chitra et al., 2017), chemiluminescence (Wu et al., 2014) and electrochemical methods (Maduraiveeran et al., 2018) have been devised to analyze glucose in real samples. Among these techniques, electrochemical biosensors stand out as highly promising tools and have garnered attention as point-of-care (POC) devices (Phetsang et al., 2019). Electrochemical sensors set the industry standard for glucose detection due to their attributes: low detection limits, heightened reliability, swift response times, operational simplicity and significantly lower costs compared to sensors using alternative detection mechanisms (Wei et al., 2020).

Amperometric electrochemical glucose biosensors relying on the enzyme glucose oxidase have been extensively studied for detecting glucose levels in food and blood, aiming for enhanced electrocatalytic responses and heightened sensitivity (Faisal et al., 2010). However, immobilized enzyme sensors possess certain drawbacks, including instability triggered by intrusive chemicals and alterations in sample pH and temperature. To tackle these constraints, a different approach has come to light: direct electrochemical oxidation of glucose using nonenzymatic glucose sensors (Toghill and Compton, 2010).

Functionalized nanomaterials serve various roles, functioning as catalysts, immobilization platforms or electro-optical labels, significantly boosting detection sensitivity and specificity (Rathod et al., 2010). The advent of nonenzymatic electrodes, relying on the direct electro-oxidation of glucose, marks the potential for the fourth generation of glucose sensors. These sensors are crafted by integrating nanostructured metals (Bai et al., 2010) or metal oxides (Zhang et al., 2012) onto the electrode surface, displaying markedly enhanced electrocatalytic activity towards glucose, compared to enzyme-based counterparts.

Recently, the scientific community has shifted its focus towards metal oxides, garnering significant attention as promising materials for glucose detection. This interest is primarily attributed to their notably lower costs and enhanced resistance to poisoning and fouling (Zhu et al., 2016). Particularly, NiO (Franceschini and Taurino, 2022), CuO (Ashok et al., 2019) and their composites (Wei et al., 2021) have emerged as prominent candidates, often featuring surface nanostructuring. Additionally, ongoing investigations are exploring oxides such as Co_3O_4, FeO_x and MnO_x (Sattarahmady and Heli, 2012), (Si et al., 2013), (Raza and Ahmad, 2018).

Among the transition series, vanadium and its oxides (VO_x) stand out as incredibly diverse and intriguing catalytic systems. Their applications range from synthesizing vital chemicals (Wachs, 2013) to reducing environmental pollutants (Monfort and Petriskova, 2021) and more recently, being employed in neuromorphic and switching devices (Li et al., 2022). The complexity of their chemistry can be attributed to two primary factors: the multitude of oxidation states in which vanadium can exist (ranging from V^{2+} to V^{5+}) and the varied coordination geometry of oxygen ions. Additionally, these oxides possess a noteworthy ability to create mixed-valence oxides through the inclusion of oxygen vacancy defects (Berenguer et al., 2017). These defects have been found to enhance the adsorption of specific reactants, ultimately catalyzing numerous oxidation or reduction reactions (Kämper et al., 2000).

In disease monitoring applications, screen-printed electrodes (SPEs) hold an edge over other electrode types due to their adaptability for modification, diverse material composition, varied geometries, compact sizes, affordability, simplicity and portability. Therefore, the combination of screen-printing technology with inexpensive nanomaterials holds great promise for crafting biosensing devices. Such devices can operate with minimal sample volumes while showcasing excellent selectivity and sensitivity in their responses (Chu et al., 2017).

This study involves modifying a screen-printed gold electrode through electrochemical deposition of V_2O_5 nanoparticles, followed by activation in an alkaline medium to create SPGE/V_2O_5. The aim was to establish a straightforward sensing platform utilizing the modified electrode as a glucose biosensor. This research work illustrated the creation, classification and establishment of a D-glucose sensor utilizing SPGE/V_2O_5 using cyclic voltammetry as the method of choice.

Experimental

Materials

The substances employed in this research, including vanadium pentoxide, hydrogen peroxide, sodium hydroxide, glucose, ascorbic acid, fructose and maltose were sourced from Sigma-Aldrich Corp. (USA) and met analytical grade standards. Alkaline solutions were prepared using NaOH pellets and all solutions were made using deionized water. The tests were conducted under typical room temperature conditions. Screen printed gold electrodes (SPGE) were obtained from Metrohm DropSens S.L. (Spain).

Construction of the V_2O_5 Non-enzymatic Glucose Sensor

The V_2O_5 film was electrochemically deposited onto the SPGE. To dissolve 0.18 g of V_2O_5 powder, a solution was prepared by vigorously stirring it with 10 mL of deionized water and 0.9 mL of 30% hydrogen peroxide for 1 hour at room temperature. Twenty microliters (20 µL) of this electrolyte solution was applied onto the SPGE. Employing a pulsed electrodeposition technique, initially, the electrode potential was set at 0 V for 20 seconds to achieve equilibrium. Subsequently, it was adjusted to -2.0 V for 10 seconds to aid in the electrophoretic deposition of V_2O_5. This cycle was iterated 60 times (Uchaker et al., 2014).

Glucose solutions ranging from 1 mM to 10 mM were prepared in a 0.1 M NaOH solution. As the glucose concentration increased, anodic peak current rose notably at around +0.7 V due to the interaction between glucose and V_2O_5 in an alkaline solution. To utilize the V_2O_5-based sensor, 20 µL of a known glucose solution in 0.1 M NaOH was drop-casted. A 10-second resting period allowed hydroxide ions to initiate V_2O_5 oxidation. Subsequently, cyclic voltammetry (CV) was performed between -1.0 and +1.0 V. The mechanism of the glucose sensor is proposed in Scheme 1.

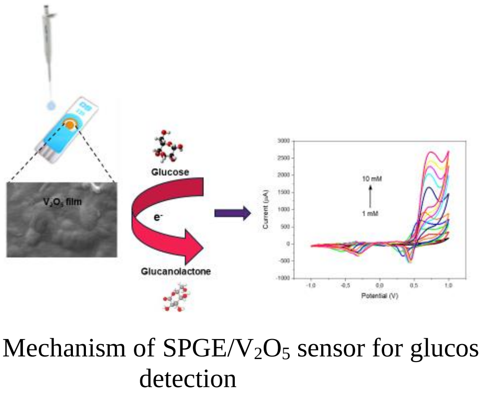

Scheme 1. Mechanism of SPGE/V_2O_5 sensor for glucose detection

Instrumentation

Electrochemical evaluations were performed with a Metrohm Dropsens µStat-i potentiostat/galvanostat, employing screen-printed gold electrodes obtained from Metrohm DropSens (Spain). These electrodes comprised a 3-electrode electrochemical cell, including gold-based working and counter electrodes, a quasi-reference electrode made of silver and electrical contacts. The working electrode had a diameter of 4 mm. A DRP-DSC connector facilitated the connection between the screen-printed electrodes and the potentiostat. CV experiments were executed at a scan rate of 100 mVs^{-1} within the potential range of -1.0 to +1.0 V to evaluate the electrochemical behavior of each sample. For morphological analysis of the V_2O_5-modified electrodes, a LS10 scanning electron microscope (SEM) (Zeiss Evo, Carl Zeiss NTS, Germany) was utilized, outfitted with an energy-dispersive X-ray spectroscopy (EDX) analysis detector (Zeiss Evo). The structural analysis was conducted utilizing a D8 Advance X-ray Diffractometer (XRD) (Bruker, Germany), operating within the 2θ range of 10-60° with a scan rate of 2°/min.

Results and Discussion

SEM images of bare and V_2O_5 modified SPGE are presented in Fig 1a and 1b, respectively. As shown in Fig. 1a, bare SPGE has a porous structure whereas the V_2O_5 SEM image depicts a rough surface marked by prominent globular structures as indicated in Fig 1b. Figure 1c displays the XRD pattern of V_2O_5 film. The XRD analysis reveals a preferential orientation in the V_2O_5 thin film, aligning with the (001) plane at a 2Θ angle of 20.33. This orientation indicates a single phase consistent with the diffraction data JCDPS file No. 41-1426, confirming the orthorhombic structure of V_2O_5 (Berouaken et al., 2022).

Elemental analysis through EDX and mapping of elements verified the chemical composition of V_2O_5, confirming the presence of vanadium (V) and oxygen (O) elements. These elements were distinctly visible in the EDX spectrum of V_2O_5 (Fig. 1d). The amounts of vanadium (V) and oxygen (O) elements were found to be 17.54% and 82.46%, respectively according to EDX analysis. The homogeneous dispersion of elements V and O on the V_2O_5 electrode's surface is illustrated in Fig. 1(e-g) through elemental mapping images, where green and blue colors symbolize each respective element.

CV was employed to assess the electron transfer behavior exhibited by different modified electrodes including the bare SPGE and V_2O_5-modified SPGE electrodes, both before and after the incorporation of glucose into a 0.1 M NaOH solution. The experiment encompassed a potential range from -1.0 to +1.0 V, with a scan rate set at 100 mV s^{-1} and the resulting CVs are depicted in Fig. 2. Notably, the unmodified SPGE electrode displayed no discernible redox peaks within the assessed potential range. In contrast, all modified electrodes exhibited well-defined redox response peaks, indicating distinct interfacial structures that significantly influenced the observed electrochemical responses (Phetsang et al., 2019).

In the absence of glucose, the cyclic voltammogram (CV) exhibited a pair of anodic and cathodic peaks centered around +0.6 and -0.3 V, attributed to the oxidation/reduction reactions of vanadium species. This observation confirmed the effective activation of the electrode for sensing purposes. Upon the addition of glucose to the electrolyte solution, there was an increase in the anodic peak current linked to the augmentation of vanadium species. Additionally, a slight shift to higher potentials was noted, indicating the electrocatalytic mechanism of glucose oxidation facilitated by V_2O_5. In the proposed electrocatalytic reaction mechanism elucidating D-glucose with V_2O_5 through the I–V performance, the electro-oxidation of D-glucose resulted in its transformation into D-gluconolactone, which then converted into D-gluconic acid and hydrogen peroxide. Subsequently, H_2O_2 was converted into oxygen and protons, liberating two electrons. These released electrons were reflected in the current–voltage curve, enabling the detection of D-glucose (Rinaldi and Carballo, 2016).

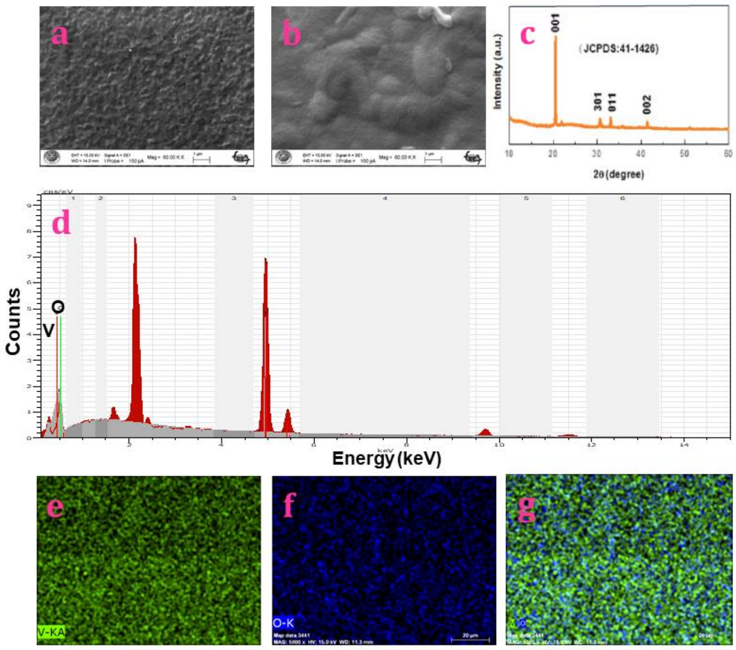

Figure 1. a) SEM image of bare SPGE b) SEM image of SPGE/V_2O_5 c) XRD pattern of V_2O_5 d) EDX spectrum of V_2O_5 e-g) Elemental mapping of V_2O_5 e) vanadium (green) f) oxygen (blue) g) overall mapping

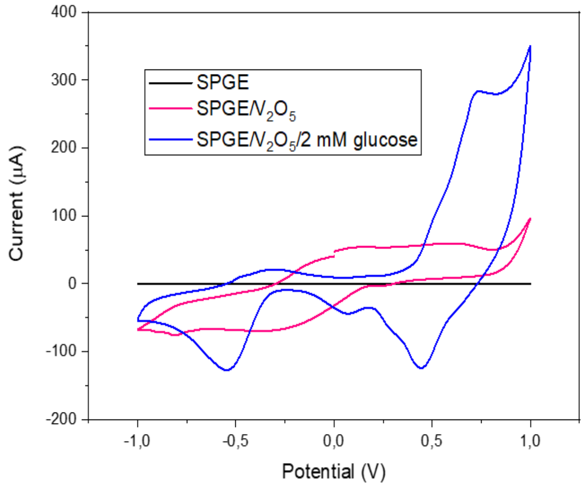

Figure 2. CV curves of SPGE and V_2O_5 modified SPGEs before and after addition of 2 mM glucose in 0.1 M NaOH solution at the scan rate of 100 mV s^{-1}

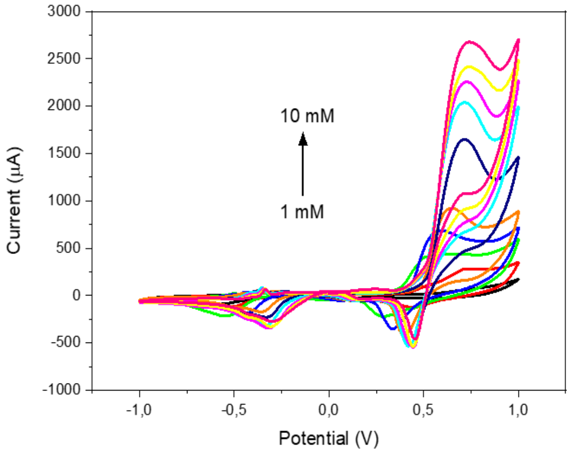

Figure 3. CV curves of V_2O_5 modified SPGE under various glucose concentration from 1 mM to 10 mM in 0.1 M NaOH solution at the scan rate of 25 mV s^{-1}

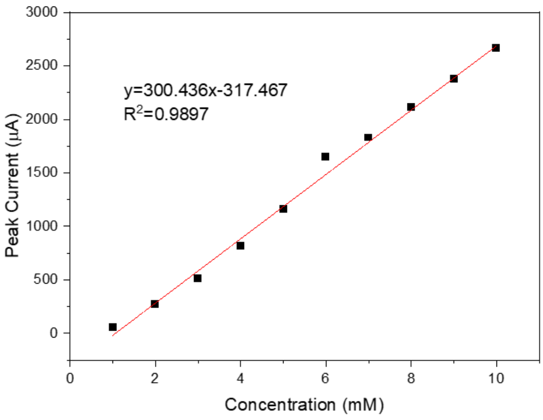

Figure 4. Calibration plot between the anodic peak currents vs glucose concentration

The observed phenomenon can be attributed to limitations arising from glucose absorption, potential intermediate presence and diffusion challenges within the diffusion layer. These factors collectively hinder the kinetics of the overall reaction, resulting in the positive shift observed in the anodic current. Furthermore, the accompanying figure demonstrates two cathodic peaks at +0.44 and -0.54 V following glucose addition, affirming both the outstanding electrocatalytic capabilities of the SPGE/V_2O_5 electrode and the irreversible nature of glucose oxidation (Fernandez et al., 2020).

The oxidation of sugars involves a dehydrogenation reaction, where the reactive group is typically a hemiacetal group found in all reducing sugars. It is proposed that the electrocatalysis process typically involves the attachment of the analyte onto the electrode surface, likely engaging d-electrons and vacant d-orbitals of the metallic substrate. Thus, it's highly likely that the adsorption of sugars onto the catalyst plays a pivotal role in initiating the oxidation reaction (Pérez-Fernández et al., 2016).

The SPGE/V_2O_5 electrode's sensing capability was monitored using CV. As illustrated in the Figure 3, each incremental addition of glucose correlated with an amplified CV signal. Within the 1–10 mM range, there existed a linear correlation between glucose concentration and the CV signal, demonstrating a detection limit of 0.9 µM. These performance metrics either match or occasionally surpass those previously reported in similar studies.

In summary, the process begins with the electrochemical uptake of glucose onto the SPGE/V_2O_5, followed by a dehydrogenation step. V_2O_5 film, formed at higher anodic potentials, significantly enhances the catalytic effect on glucose oxidation. The adsorbed glucose molecule can undergo direct oxidation to form gluconate, releasing OH^- along with the elimination of H^+. Alternatively, another pathway involves the conversion of dehydrogenated glucose into gamma-gluconolactone through oxidation, which further transforms into gluconate upon reacting with hydroxide ions. The electrode current's magnitude depends heavily on both the concentration of glucose and the pH of electrolyte, specifically the quantity of OH^- ions, as these ions are essential to counterbalance the protons produced in the dehydrogenation phase of the reaction (Grochowska et al., 2019). NaOH serves as a widely used electrolytic medium for non-enzymatic electrochemical sugar detection due to its crucial role demonstrated by OH^- ions in the reaction (Luo et al., 1996).

The oxidation peak current density observed during the reverse scan gradually rises with rising glucose content in the electrolyte. A graphical representation of the relationship between current (I) and concentration (c) was depicted in Fig.4. At lower glucose levels, a direct relationship between glucose concentration and current was established. Utilizing the equation: 3SD/slope (where SD denotes standard deviation and slope is obtained from the linear regression model) (Grochowska et al., 2019), a low detection limit of 0.9 µM was calculated.

Investigating interference effects is crucial in analytical science because it enables the distinction between interfering elements and a biomolecule with a similar physiological context within the biosensor. The sensor's selectivity was probed through CV using a consistent glucose concentration. The assessment focused on discerning the impact of various species that might disrupt sugar determination due to their close proximity in oxidation processes. Ascorbic acid, fructose and maltose were specifically studied as potential interfering species commonly found in food samples, usually at lower concentrations compared to sugars (Pérez-Fernández et al., 2016).

Figure 5a and 5b illustrate the electrode material's electrochemical response to various interfering species. When successively introduced into a 10 mM glucose solution, ascorbic acid, fructose and maltose showed notable differences in the current density of the oxidation peak recorded at +0.7 V.

As depicted in the Figures 5a and 5b, the interfering molecules undergo oxidation at the applied operational potential of +0.7 V. The current outputs resulting from the electrochemical oxidation of these interfering species might influence the analytical responses for glucose determination (Phetsang et al., 2019). Additionally, as observed in the Fig 5, the introduction of these mentioned interferences doesn't yield an increase in peak height at the glucose oxidation peak position in the CV profile, demonstrating the favorable selectivity of the resulting sensor (Hallaj et al., 2020).

In comparison to various non-enzymatic glucose sensors predominantly evaluated in alkaline environments, the performance of this glucose sensor matches or, in many instances, surpasses that of previously reported works, as detailed in Table 1.

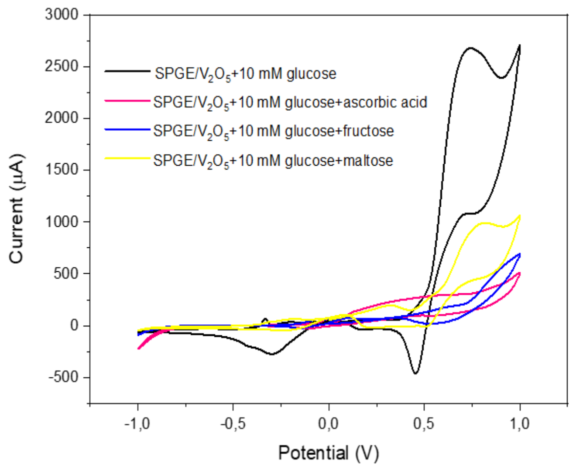

Figure 5a. The impact of biomolecules on interference

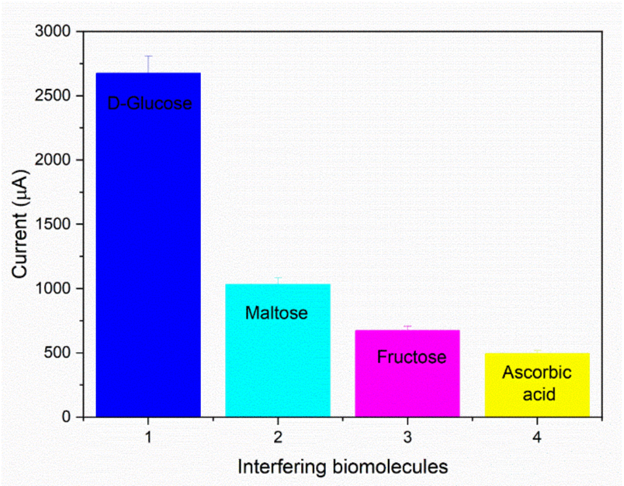

Figure 5b. Bar graph depicting the interference effect at +1.0 V

Table 1. Assessing the analytical performance of our proposed glucose sensor compared to various modified electrodes reported for glucose determination.

Catalyst	Morphology	Electrode	Chemical Environment	Linear range	Limit of detection	Selectivity	Ref
NiO	Hollow microsphere	GCE	0.1 M NaOH	0.005-0.364 mM	2 µM	AA, Urea, Leu, Pro, Lys, NaCl	(Cui et al., 2015)
Cu_2O	Nanoparticle	VC/graphite disk	0.1 M KOH	0-6 mM	2.4 µM	AA, KCl	(El Khatib and Hameed, 2011)
Co_3O_4	Nanofiber	GCE	0.1 M NaOH	0-2.04 mM	0.97 µM	AA, UA	(Ding et al., 2010)
Fe_2O_3	Nanoparticle	GCE	0.1 M PBS	0.0025-0.58 mM	0.58 µM	AA, UA	(Chen et al., 2014)
Mn_3O_4	Nanomesh	3D GF	0.1 M NaOH	0.1-8 mM	10 µM	AA, UA, AP	(Si et al., 2013)
$ZnO.V_2O_5$	Nanorod	GCE	100 mM PBS	1-1000 µM	125 250 µM	AA, Fruc, Dopamine, UA	Rahman et al., 2019
VO_x	Thin film	GCE	0.1 M KOH	1-10 mM	0.32 mM	AA, Acetominophen	Franceschini et al.,2023
V_2O_5@GO	Nanoparticle	Gold electrode	0.01 M NaOH	0.5-7.5 mM	0.859 mM	-	Prabakaran et al., 2024
V_2O_5	Thin film	SPGE	0.1 M NaOH	1-10 mM	0.9 µM	AA, Fruc, Malt	this work

Conclusion

A straightforward potentiostatic approach successfully enabled the preparation of a V_2O_5 thin film on the SPGE surface. This deposition technique facilitated the creation of well-dispersed V_2O_5 nanostructures on the electrode, significantly enhancing its electrocatalytic process in glucose oxidation during electrochemical assessments. These findings underscore the potential of V_2O_5 nanostructures as exceptional electrode materials for glucose sensing applications. The V_2O_5-modified SPGE exhibited an extensive linear range spanning 1 mM to 10 mM, boasting a detection limit as low as 0.9 μM for glucose. Notably, common interfering species found in physiological environments showed no discernible impact on glucose oxidation using SPGE/V_2O_5 electrodes. This suggests promising prospects for SPGE/V_2O_5 electrodes in non-enzymatic glucose sensing applications. Moreover, this study sheds light on the fascinating electrocatalytic behavior of V_2O_5 thin films and introduces electrodeposition as a safe and viable deposition method for V-based glucose electrocatalysts, marking a pioneering exploration in this field.

References

Ashok A., Kumar A., & Tarlochan F. (2019). Highly efficient nonenzymatic glucose sensors based on Dendritic core-shell copper-nickel alloy@metal oxide for efficient non-enzymatic glucose detection CuO nanoparticles. *Applied Surface Science,* 481, 712-722. https://doi.org/10.1016/j.apsusc.2019.03.157

Bai H., Han M., Du Y., Bao J., & Dai Z. (2010). Facile synthesis of porous tubular palladium nanostructures and their application in a nonenzymatic glucose sensor. *Chemical Communications* 46(10), 1739– 1741. https://doi.org/10.1039/B921004K

Berenguer R., Guerrero-Pérez M. O., Guzmán I., Rodríguez-Mirasol J., & Cordero T. (2017). Synthesis of Vanadium Oxide Nanofibers with Variable Crystallinity and V^{5+}/V^{4+} Ratios. *ACS Omega,* 2, 7739-7745. https://doi.org/10.1021/acsomega.7b01061

Berouaken M., Yaddaden C., Ferdjouni H., Torki C., Maoudj M., Chebout K., Ayat M., Menari H., Manseri A., & Gabouze N. (2022). Investigation of hybrid nanostructure based on nanorods vanadium pentoxide/mesoporous silicon as electrode materials for electrochemical supercapacitor. *Applied Physics A,* 128, 653. https://doi.org/10.1007/s00339-022-05804-6

Chen Y. X., Zhang H. H., Xue H. G., Hu X. Y., Wang G. X., & Wang C. Y. (2014). Construction of a non-enzymatic glucose sensor based on copolymer P4VP-co-PAN and Fe_2O_3 nanoparticles. *Materials Science&Engineeering C,* 35, 420-425. https://doi.org/10.1016/j.msec.2013.11.030

Chitra J., Ghosh M., & Mishra H.N. (2017). Rapid quantification of cholesterol in dairy powders using Fourier transform near infrared spectroscopy and chemometrics. *Food Control,* 78, 342–349. https://doi.org/10.1016/j.foodcont.2016.10.008

Chu Z., Peng J., & Jin W. (2017). Advanced nanomaterial inks for screen-printed chemical sensors. *Sensors and Actuators B Chemical,* 243, 919–926. https://doi.org/10.1016/j.snb.2016.12.022

Cui Z. Z, Yin H. Y., Nie Q. L., Qin D. Y., Wu W. W., & He X. L. (2015). Hierarchical flower-like NiO hollow microspheres for non-enzymatic glucose sensors. *Journal of Electroanalytical Chemistry,* 757, 51-57. https://doi.org/10.1016/j.jelechem.2015.09.011

Dhara K., & Mahapatra D.R. (2018). Electrochemical nonenzymatic sensing of glucose using advanced nanomaterials. *Microchimica Acta,* 185, 49. https://doi.org/10.1007/s00604-017-2609-1

Ding Y., Wang Y., Su L. A., Bellagamba M., Zhang H., & Lei Y. (2010). Electrospun Co_3O_4 nanofibers for sensitive and selective glucose detection. *Biosensors&Bioelectronics,* 26, 542-548. https://doi.org/10.1016/j.bios.2010.07.050

Dong Q., Ryu H., & Lei Y. (2021). Metal oxide based non-enzymatic electrochemical sensors for glucose detection. *Electrochimica Acta,* 370, 137744. https://doi.org/10.1016/j.electacta.2021.137744

El Khatib K. M., & Hameed R. M. A. (2011). Development of Cu_2O/Carbon Vulcan XC-72 as non-enzymatic sensor for glucose determination. *Biosensors&Bioelectronics,* 26, 3542-3548. https://doi.org/10.1016/j.bios.2011.01.042

Faisal S.N., Pereira C.M., Rho S., & Lee H.J. (2010). Amperometric proton selective sensors utilizing ion transfer reactions across a microhole liquid/gel interface. *Physical Chemistry Chemical Physics,* 12, 15184–15189. https://doi.org/10.1039/C0CP00750A

Fernandez I., Gonzalez-Mora J. L., Lorenzo-Luis P., Villalonga R., & Salazar-Carballo P. A. (2020). Nickel oxide nanoparticles-modified glassy carbon electrodes for non-enzymatic determination of total sugars in commercial beverages. *Microchemical Journal,* 159, 105538. https://doi.org/10.1016/j.microc.2020.105538

Filip M., Vlassa M., Coman V., & Halmagyi A. (2016). Simultaneous determination of glucose, fructose, sucrose and sorbitol in the leaf and fruit peel of different apple cultivars by the HPLC–RI optimized method. *Food Chemistry,* 199, 653–659. https://doi.org/10.1016/j.foodchem.2015.12.060

Franceschini F., & Taurino I. (2022). Nickel-based catalysts for non-enzymatic electrochemical sensing of glucose: A review. *Physics in Medicine,* 14, 100054. https://doi.org/10.1016/j.phmed.2022.100054

Franceschini F., Payo M. R., Schouteden K., Ustarroz J., Locquet J. P., & Taurino I. (2023). MBE Grown Vanadium Oxide Thin Films for Enhanced Non-Enzymatic Glucose Sensing. *Advanced Functional Materials,,* 2304037. https://doi.org/10.1002/adfm.202304037

Grochowska K., Ryl J., Karczewski J., Śliwiński G., Cenian A., & Siuzdak K. (2019). Non-enzymatic flexible glucose sensing platform based on nanostructured TiO_2–Au composite. *Journal of Electroanalytical Chemistry,* 837, 230-239. https://doi.org/10.1016/j.jelechem.2019.02.040

Hallaj R., Mohammadian N., Ghaderi S., & Navae A. (2020). Nonenzymatic and low potential glucose sensor based on electrodeposited Ru-nanofilm from ionic liquid electrolyte. *Materials Science and Engineering: B,* 261, 114666. https://doi.org/10.1016/j.mseb.2020.114666

Kämper A., Hahndorf I., & Baerns M. (2000). A molecular mechanics study of the adsorption of ethane and propane on V_2O_5(001) surfaces with oxygen vacancies. *Topics in Catalysis,* 11, 77-84. https://doi.org/10.1023/A:1027239612464

Li G., Xie D., Zhong H., Zhang Z., Fu X., Zhou Q., Li Q., Ni H., Wang J., Guo Er-J, He M., Wang C., Yang G., Jin K., & Ge C. (2022). Photo-induced non-volatile VO_2 phase transition for neuromorphic ultraviolet sensors. *Nature Communications,* 13, 1729. https://doi.org/10.1038/s41467-022-29456-5

Luo P. F., Kuwana T., Paul D. K., & Sherwood P. M. (1996). Electrochemical and XPS Study of the Nickel-Titanium Electrode Surface. *Analytical Chemistry,* 68, 3330–7. https://doi.org/10.1021/ac960236e

Maduraiveeran G., Sasidharan M., & Ganesan V. (2018). Electrochemical sensor and biosensor platforms based on advanced nanomaterials for biological and biomedical applications. *Biosensors& Bioelectronics,* 103, 113–129. https://doi.org/10.1016/j.bios.2017.12.031

Monfort O., & Petrisková P. (2021). Binary and Ternary Vanadium Oxides: General Overview, Physical Properties, and Photochemical Processes for Environmental Applications. *Processes,* 9, 214. https://doi.org/10.3390/pr9020214

Pérez-Fernández B., Martín-Yerga D., & Costa-García A. (2016). Electrodeposition of nickel nanoflowers on screen-printed electrodes and their application to non-enzymatic determination of sugars. *RSC Advances,* 6, 83748-83757. https://doi.org/10.1039/C6RA15578B

Phetsang S., Jakmunee J., Mungkornasawakul P., Laocharoensuk R., & Ounnunkad K. (2019). Sensitive amperometric biosensors for detection of glucose and cholesterol using a platinum/reduced graphene oxide/poly(3-aminobenzoic acid) film-modified screen-printed carbon electrode. *Bioelectrochemistry,* 127, 125–135. https://doi.org/10.1016/j.bioelechem.2019.01.008

Prabakaran L., Shankar P., Kulinich S. A, & Balaguru Rayappan J. B. (2024). Eco-friendly fabrication of V_2O_5@GO hybrids for direct glucose electrooxidation and sensing: An alternative to noble metals. *Journal of Industrial and Engineering Chemistry,* 132, 383–394. https://doi.org/10.1016/j.jiec.2023.11.032

Rahman M.M., Hussain M.M., & Asiri A. M. (2019). D-Glucose sensor based on ZnO.V_2O_5 NRs by an enzyme-free electrochemical approach. *RSC Advances,* 9, 31670. https://doi.org/10.1039/C9RA06491E

Rathod D., Dickinson C., Egan D., & Dempsey E. (2010). Platinum nanoparticle decoration of carbon materials with applications in non-enzymatic glucose sensing. *Sensors and Actuators B Chemical* 143(2), 547–554. https://doi.org/10.1016/j.snb.2009.09.064

Raza W., & Ahmad K. (2018). A highly selective Fe@ZnO modified disposable screen printed electrode based non-enzymatic glucose sensor (SPE/Fe@ZnO). *Materials Letters,* 212, 231-234. https://doi.org/10.1016/j.matlet.2017.10.100

Razak K. A., Neoh S. H., Ridhuan N. S. & Nor N. M. **(**2016). Effect of platinum-nanodendrite modification on the glucose-sensing properties of a zinc-oxide-nanorod electrode. *Applied Surface Science,* 380, 32–39. https://doi.org/10.1016/j.apsusc.2016.02.091

Rinaldi A. L., & Carballo R. (2016). Impedimetric non-enzymatic glucose sensor based on nickel hydroxide thin film onto gold electrode. *Sensors and Actuators B Chemical,* 228, 43–52. https://doi.org/10.1016/j.snb.2015.12.101

Sattarahmady N., & Heli H. (2012). A non-enzymatic amperometric sensor for glucose based on cobalt oxide nanoparticles. *Journal of Experimental Nanoscience,* 7, 5, 529–546. http://dx.doi.org/10.1080/17458080.2010.539275

Si P., Dong X. C., Chen P., & Kim D. H. (2013). A hierarchically structured composite of Mn_3O_4/3D graphene foam for flexible nonenzymatic biosensors. *Journal of Materials Chemistry B,* 1, 110-115. https://doi.org/10.1039/C2TB00073C

Si P., Dong X.-C., Chen P., & Kim D.-H. (2013). A hierarchically structured composite of Mn_3O_4/3D graphene foam for flexible nonenzymatic biosensors. *Journal of Materials Chemistry B,* 1, 110-115. https://doi.org/10.1039/C2TB00073C

Toghill K.E., & Compton R.G. (2010). Electrochemical non-enzymatic glucose sensors: a perspective and an evaluation. *International Journal of Electrochemical Science,* 5, 1246–1301.

Uchaker E., Zheng Y.Z., Li S., Candelaria S.L., Hu S., & Cao G.Z. (2014). Better than Crystalline: Amorphous Vanadium Oxide for Sodium Ion Batteries. *Journal of Materials Chemistry,* 2, 18208–18214. https://doi.org/10.1039/C4TA03788J

Wachs I. E. (2013). Catalysis science of supported vanadium oxide catalysts. *Dalton Transactions,* 42, 11762-11769. https://doi.org/10.1039/C3DT50692D

Wei H., Xue Q., Li A., Wan T., Huang Y., Cui D., Pan D., Dong B., Wei R., Naik N., & Guo Z. (2021). Dendritic core-shell copper-nickel alloy@metal oxide for efficient non-enzymatic glucose detection. *Sensors and Actuators B Chemical,* 337, 129687. https://doi.org/10.1016/j.snb.2021.129687

Wei M., Qiao Y., Zhao H., Liang J., Li T., Luo Y., Lu S., Shi X., Lu W., & Sun X. (2020). Electrochemical non-enzymatic glucose sensors: recent progress and perspectives. *Chemical Communications,* 56, 14553-14569. https://doi.org/10.1039/D0CC05650B

Wu X., Chai Y., Yuan R., Zhong X., & Zhang J. (2014). Synthesis of multiwall carbon nanotubes-graphene oxide-thionine-Au nanocomposites for electrochemiluminescence detection of cholesterol. *Electrochimica Acta,* 129, 441–449. https://doi.org/10.1016/j.electacta.2014.02.103

Zhang, Y. Wang Y., Jia J., & Wang J. (2012). Nonenzymatic glucose sensor based on graphene oxide and e Y.lectrospun NiO nanofibers. *Sensors and Actuators B Chemical,* 171-172, 580–587. https://doi.org/10.1016/j.snb.2012.05.037

Zhu H., Li L., Zhou W., Shao Z., & Chen X. (2016). Advances in non-enzymatic glucose sensors based on metal oxides. *Journal of Materials Chemistry B,* 4, 7333-7349. https://doi.org/10.1039/C6TB02037B